



## Segmentation and Somitogenesis Derived from Phase Dynamics in Growing Oscillatory Media

MADS KÆRN\*§, MICHAEL MENZINGER\* AND AXEL HUNDING†

\**Department of Chemistry, University of Toronto, Toronto, ONT, Canada, M5S 3H6*  
and †*Department of Chemistry, University of Copenhagen, DK-2100 Copenhagen, Denmark*

(Received on 28 January 2000, Accepted in revised form on 30 August 2000)

The formation of spatially repetitive structures along the growth axis of a developing embryo is a common theme in developmental biology. Here we apply the novel flow-distributed oscillator (FDO) mechanism of wave pattern formation to the problem of axial segmentation in general and to somitogenesis in particular. We argue that the conditions for formation of FDO waves are satisfied during somitogenesis in the chick and mouse and that the waves of gene expression observed in these species arise from phase dynamics in a growing oscillatory medium. We substantiate this claim by showing that the FDO mechanism allows the waves to be mimicked by an inorganic experiment and that it predicts a wavelength that coincides with that observed experimentally. To see whether the FDO mechanism is compatible with other aspects of somitogenesis, we construct an FDO-based model of somitogenesis and successfully test it against a number of experimental observations, including the effect of heat shock. Our analysis provides a rigorous physical basis for the hypothesis that the phase dynamics of a segmental clock controls important stages of segmentation during somitogenesis in the chick and mouse as well as in other organisms that undergo segmentation during their axial growth.

© 2000 Academic Press

### 1. Introduction

The analysis of generic mechanisms that govern the formation of segments in a collection of identical cells has two aspects. One is the identity and function of segment-defining genes and their conservation within and across phyla. The second is the mechanism that allows for spatially localized expression of these genes. While segmentation and the associated morphological changes evidently require segment-defining genes, the machinery needed to express such genes does not on its own provide the ability to organize their expression in spatial patterns. A comprehensive

understanding of biological segmentation hence requires knowledge of the identity and function of segment-defining genes as well as a clear understanding of the mechanism(s) of spatial self-organization that allows patterns to form in a collection of identical cells. The same basic mechanism of spatial self-organization may be utilized in diverse biological systems. Hence, phenomenological mechanisms of self-organization are ideally independent of species- or phyla-specific genetic data and are ultimately capable of producing periodic patterns also in inorganic systems based on basic physico-chemical, dynamic principles.

Here we present an experimental and theoretical investigation of a novel mechanism of

§Author to whom correspondence should be addressed.  
E-mail: mkaern@alchemy.chem.utoronto.ca

self-organization that may provide axially growing organisms with the ability to express segment-defining genes in spatial patterns. It predicts a segmental program that is observed in many vertebrates, arthropods and annelids, and in some cases of limb formation where segments are formed one after the other along the growth axis. A similar program is frequently observed during phyllotaxis where leaves are generated at regular intervals within the apical meristem and the plant develops repetitive structural modules one after the other as it elongates (Wolpert, 1999). Our study is based on the recent discovery (Andrésén *et al.*, 1999; Kærn & Menzinger, 1999) of a physical mechanism capable of producing stationary and traveling phase waves, also referred to as kinematic waves or pseudo-waves (Thoenes, 1973; Kopell & Howard, 1973; Winfree, 1980; Mikhailov, 1990; Polezhaev, 1995), in open flows of oscillatory chemical media. In essence, wave patterns arise from spatio-temporal recurrence of oscillation phase when an oscillating medium is carried through space by a flow. We therefore named it the flow-distributed oscillator (FDO) mechanism (Kærn & Menzinger, 1999, 2000a, b). The FDO mechanism is *universal* in the sense that it relies only on phase dynamics and is independent of how the oscillation is generated and of the nature of the oscillating medium (Mikhailov, 1990). It therefore leads to wave pattern formation in any physical, chemical or biological system satisfying the conditions of (1) a uniform flow, of (2) oscillating elements, subject to (3) upstream temporal organization (boundary forcing).

These three conditions may be satisfied in many biological systems. There is on one hand, an increasing evidence that oscillating processes or clocks are important in early development (Sassone-Corsi, 1998) and that phase dynamics plays a key role in segmentation, as predicted by several authors (see e.g. Goodwin & Cohen, 1969; Cooke & Zeeman, 1976; Winfree, 1980; Meinhardt, 1982). On the other hand, axial growth is equivalent to an open flow. To appreciate this equivalence, consider the axial growth processes illustrated in Fig. 1. Figure 1(a) shows a growing embryo, e.g. the root or shoot of a plant, the limb bud of a vertebrate or the terminal growth zone of an annelid or an arthropod. The gray

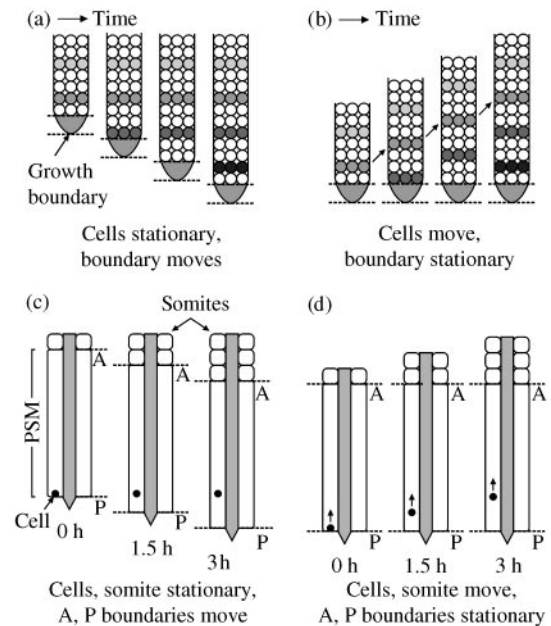


FIG. 1. Equivalence of axial growth to an open flow. Panel (a) and (b): Daughter cells (three per generation) are shed from a terminal growth zone. Every third generation is shaded to guide the eye. Panel (a) shows the reference frame where cells remain stationary and the growth zone and boundary move in the posterior (downward) direction. Panel (b) shows the same process in the reference frame where the growth zone and boundary are stationary. In this case, cells move anteriorly (upward) corresponding to a flow of cells away from the growth boundary. Panel (c) and (d): Somitogenesis as observed in many vertebrates. Panel (c) shows the reference frame where cells and somites are stationary and the anterior (labeled A) and posterior (labeled P) PSM boundaries move as the result of anterior somite formation and posterior addition of cells. A cell added to the posterior PSM boundary (black dot) is transported away from the posterior boundary due to posterior PSM growth. Panel (d) shows somitogenesis in the reference frame where the PSM boundaries remain stationary. In this case, posterior PSM growth creates a steady flow of cells through the PSM in an anterior direction.

apical area represents the proliferation zone of the dividing stem cells, whose daughter cells (symbolized here by three circles per generation) are shed axially, pushing the growth zone and boundary downward. As a result, the daughter cells and the rest of the growing form remain stationary relative to the embryo as a whole while the growth boundary moves. The stationarity of the daughter cells is emphasized by shading every third generation. Figure 1(b) shows the same developmental process with a different choice of reference frame. This figure illustrates

the axial growth in the reference frame in which the growth zone and boundary are stationary. Now the daughter cells move away from the growth boundary [upward in Fig. 1(d)] and through the developing form, as indicated by arrows. Hence, axial growth can be described equivalently by a flow of daughter cells away from the (stationary) proliferation zone. It is not important whether it is the cells or the growth boundary that actually move since motion is relative in terms of the reference frames. Axial growth and open flows are equivalent processes in the sense that both cause the distance between a cell and the growth/flow boundary to increase with time.

Figures 1(c) and (d) show how a growth-induced flow arises in many vertebrates, such as the chick and mouse, during the early developmental process of somitogenesis (reviewed by Gossler & Hrabê de Angelis, 1998). The figures also show the formation of metameric blocks of differentiated mesodermal tissue, the somites, from unsegmented cells within the presomitic mesoderm (PSM). Somites arise periodically (every 90 min in the chick) on either side of the neural tube [gray in Fig. 1(c) and (d)] at the anterior (upper) end of the PSM. While cells are incorporated into the somites and are removed from the PSM at its anterior boundary, the overall length of the PSM remains relatively constant since posterior addition of new cells compensates for their anterior loss. Axial growth seems to be the result of a stem cell population residing in the primitive streak (Dale & Pourquié, 2000; Stern & Vasiliasukas, 2000) but the reason for the relative constant length of the PSM remains unknown.

As shown in Fig. 1(c), it appears as if the PSM moved through the embryo with a velocity equal to the rates of posterior growth and anterior shortening while the somites and the cells within the PSM remain stationary. Figure 1(d) shows the same process in the reference frame where the posterior PSM growth boundary is stationary. In this case, cells are constantly added to its (stationary) posterior boundary and removed from its (stationary) anterior boundary, thus creating a steady flow of cells through the PSM. This growth-induced flow of cells is what allows a comparison between biological growth and chemical flow systems.

The most compelling evidence for the involvement of FDO waves in biological segmentation is provided by somitogenesis in the chick and mouse. Apart from the ubiquitous presence of axial PSM growth/flow, recent experiments (Palmeirim *et al.*, 1997) have established the involvement of a cellular “segmental clock” (Lewis, 1998) in their somitogenesis. Figure 2(a) is a schematic illustration of experimentally observed waves of *c-hairy1* mRNA expression during the

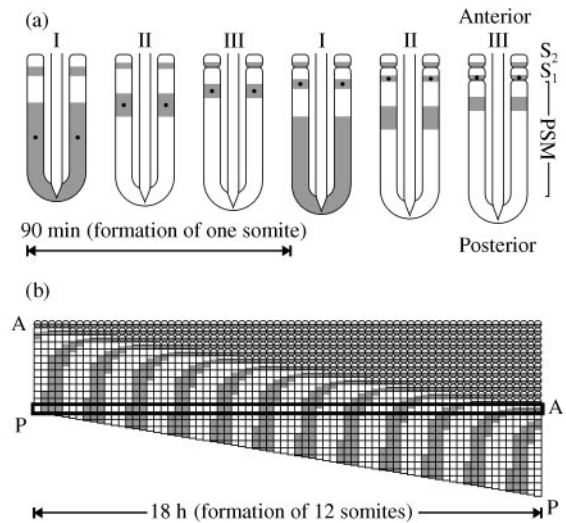


FIG. 2. Experimentally observed waves of *c-hairy1* mRNA expression during somitogenesis in the chick (based on experiments by Palmeirim *et al.*, 1997). Panel (a): gene expression waves during the formation of two somite pairs. During this time period (180 min), an expression band (shaded gray; its center is marked by a black dot) travels from the posterior (bottom) to the anterior end of the PSM. In stage I, a wide expression band is present in the posterior end of the PSM. As it travels towards the anterior end, its velocity and width decrease. The band becomes stationary when it has reached the anterior end of the PSM (stage III, second cycle), corresponding to a stationary wave with wavelength equal to one somite length  $l$ . The 90 min periodicity of somite formation equals the posterior oscillation period  $T'$ . Panel (b): Space-time plot equivalent to (a) over an 18 hr period (redrawn from Stern & Vasiliasukas, 1998). Somites (circles) are formed from prospective somites (squares) periodically at the anterior end of the PSM. As anterior cells are incorporated into somites, and thus leave the PSM, the overall length of the PSM remains constant through posterior recruitment of cells. This creates a downward (posterior) motion of the PSM. The prospective somite entering the PSM at the left (horizontal box) moves through the PSM at velocity  $v = l/T'$  and forms a somite after 18 hr. The box emphasizes that the cells within the prospective somite completes approximately 10 expression cycles before being incorporated into a somite. As evident from the homogeneous oscillation in the posterior PSM half, cells enter the PSM with temporally organized phases.

formation of two somite pairs in the chick (Palmeirim *et al.*, 1997). *Lunatic fringe* mRNA expression shows a similar spatio-temporal behavior (McGrew *et al.*, 1998; Forsberg *et al.*, 1998; Aulehla & Johnson, 1999; Barrantes *et al.*, 1999). Initially (stage I), one observes a wide expression band spanning more than half of the posterior end of the PSM. This wide band appears every 90 min and the posterior PSM halves oscillate with a constant period of 90 min. The posterior oscillation periodically initiates expression bands that traverse the PSM with decreasing velocity and width. A band comes to a stop when it reaches the anterior end of the PSM (stage III, second cycle) and shortly thereafter it is incorporated into the posterior half of the newly forming somite.

This intricate spatio-temporal behavior of gene expression waves is summarized in the space-time plot in Fig. 2(b) (redrawn from Stern & Vasiliasukas, 1998) over a longer time scale. Only one of the bilaterally symmetric PSM halves is shown. The figure also shows the downward movement of the posterior and anterior PSM boundaries and the equivalence of this movement to a flow of prospective somites (squares) through the PSM. The horizontal box outlines a prospective somite that enters the PSM at its posterior end [at the left in Fig. 2(b)] and matures into a somite (circle) at the anterior end of the PSM [at the right in Fig. 2(b)]. This group of cells is thus transported across the entire length of the PSM and each cell completes about 10 expression cycles before the gene is expressed at a constant level. The cells near the posterior boundary have synchronized gene expression and are evidently temporally organized either before or while the cells enter the PSM. The involvement of a growth-driven flow-distributed cellular oscillator subject to temporal organization at the growth boundary thus seems to be experimentally established during chick and mouse somitogenesis.

We show in this paper that the gene expression waves observed in the chick and mouse can be mimicked by a chemical flow system and that the FDO mechanism, without any additional assumptions, gives rise to a stationary wave pattern whose wavelength coincides with that observed experimentally (Fig. 2). The facts that the three

conditions seem satisfied during somitogenesis in the chick and mouse, that the mechanism reproduces observed spatio-temporal wave behavior in a chemical system and that it predicts the correct wavelength of the segmental pattern are compelling evidence for the involvement of the FDO mechanism in somitogenesis. To further substantiate this claim, we constructed a simple FDO-based model of somitogenesis. Analysis of this model shows that the FDO mechanism provides a natural explanation for the relative constant PSM length, the bilateral symmetric and synchronous segmentation of the PSM, reversed segmentation when a fragment of the PSM is inverted and the differently sized segments observed during different stages of development. We also show that the FDO model can account for the effect of heat shock and of cell cycle inhibitors and discuss in detail how the localized gene expression induced by the FDO mechanism may determine somite polarization, somite boundaries and metameric structures within the PSM.

The FDO model of somitogenesis is based on the idea that localized expression of segment-defining genes may naturally arise by an intracellular segmental clock that is coupled to axial growth. While the possibility of growth-driven segmentation was pointed out by Meinhardt (1982), phase dynamics in growing oscillatory medium has not been investigated in any detail. Most models of somitogenesis, i.e. the pendulum-escapement model by Meinhardt (1982, 1999), the clock-and-wavefront model (Cooke & Zeeman, 1976; Cooke, 1998) in its interpretation by Lewis (see Palmeirim *et al.*, 1997), the clock-and-induction model by Schnell & Maini (2000) and the clock-and-trail model by Kerszberg & Wolpert (2000), involve arrest of either the segmental clock itself or another periodic process coupled to the segmental clock. Unless the oscillation phase serves as a signal, as in the original clock-and-wavefront model and the cell-cycle model (Primm *et al.*, 1988, 1989; Collier *et al.*, 2000), a phase wave can only generate a stationary pattern in the reference frame of stationary cells if the oscillation frequency becomes (asymptotically) zero. It is therefore natural that we base our model on the slowing down and the arrest of the segmental clock.

The FDO model thus reiterates ideas proposed by several authors. Our contribution is two-fold: to explicitly incorporate and investigate the consequences of axial growth and to formulate a unified, phenomenological mechanism of wave pattern formation with a generality that allows a chemical system to mimic the spatio-temporal expression of the segmental clock genes. To the best of our knowledge, the only existing mechanism with this generality is Turing's mechanism (Turing, 1952; Castets *et al.*, 1990). In the light of its tremendous impact (see e.g. Meinhardt, 1982; Murray, 1993; Hunding & Engelhardt, 1995; Kondo & Asai, 1995; Maini *et al.*, 1997; Painter *et al.*, 1999; Hunding, 1999), it is, in our opinion, important that an alternative mechanism be substantiated analytically and that its basic physico-chemical principles be demonstrated experimentally.

This paper is organized as follows. In Section 2, we discuss the properties of biological systems that are required for the formation of spatio-temporal FDO waves and derive and verify analytic expressions for the wavelength and wave velocity for the simplest FDO waves. We then show that a chemical flow system mimics the gene expression waves observed in the chick and mouse and that the FDO mechanism accounts qualitatively and quantitatively for the observed waves. In Section 3, we describe and test the FDO-based model of somitogenesis against experimental observations and discuss how localized gene expression by the FDO mechanism may be involved in the determination of somite polarization and boundaries as well as the morphogenic structure of the PSM. Finally, in Section 4, we discuss how the FDO model relates to other models of segmentation and somitogenesis and how the FDO mechanism may provide an easy-to-exploit and economical way for an organism to express segment-defining genes in spatio-temporal patterns.

## 2. The FDO Mechanism

In this section, we explore the FDO mechanism as a mechanism of wave pattern formation in axially growing systems. The biological systems where the FDO mechanism is expected to be operational are those in which

- cells are continuously added to a growing form at a growth boundary and remain relatively stationary with respect to the overall body plan,
- certain cellular events occur periodically at intervals determined by an intracellular clock,
- the phases of the cellular oscillators are organized at or near the growth boundary such that the cells added to the structure at the same time are at the same stage of the periodic process,
- the initial synchrony is preserved such that the oscillation phase remains more or less the same in the cells added at the same time.

In its formulation for chemical flow systems, the FDO mechanism involves three parameters: the flow rate  $v$ , the intrinsic oscillation period  $T$  and the boundary forcing period  $T'$ . In biology, the meanings of the parameters are: the rate of axial extension, the period of the cellular process within the growing form and the period of the cellular process at the growth boundary. We will refer to  $v$ ,  $T$  and  $T'$  as the growth rate, the intrinsic period and the boundary period, respectively.

### 2.1. PHASE DYNAMICS

To explore the consequences of a cellular periodic process that is coupled to axial growth, we initially adopt the reference frame in which the growing boundary is stationary [Fig. 1(b) and (d)]. Consider a cell that is added to a growing biological form at the growth boundary and then moves away from it at a velocity equal to the rate of growth. As discussed in the introduction, it is not important whether it is the growth boundary or the cell that actually moves. What is important is the fact that axial growth or a flow distributes a temporal process along the growth/flow axis.

The simplest FDO waves are generated when the growth/flow rate  $v$ , the intrinsic period  $T$  and the boundary period  $T'$  are constant. In this case, growth establishes a linear relationship  $a = x/v$  between the age  $a$  of a cell, measured as the time spent in the growing form, and the distance  $x$  from the growth boundary. Hence, a linearly increasing age gradient is established along the growth axis and axial growth may encode

positional information if, for instance, an intracellular factor accumulates linearly in time. The situation becomes subtler when axial growth is coupled to an oscillatory cellular process. In this case, the oscillation phase increases linearly in time and a phase gradient is established within the growing form. The oscillation is not required to have any special shape or form but is required to be periodic such that the phase  $\phi(t)$  at time  $t$  is equal to the phase  $\phi(t + T)$  at time  $t + T$ . A simple such function is  $z = \sin(2\pi t/T)$  that advances by  $2\pi$ , i.e. one full unit cycle, when time increases from  $t$  to  $t + T$ . Measured in radians, i.e. modulo  $2\pi$ , this corresponds to  $\Delta\phi = 1$  for  $\Delta t = T$ . Real oscillatory processes generally do not have the simple symmetrical shape of a sine function. One can however always monitor the progression through the oscillation in terms of a phase that increases linearly in time such that the phase advances by one ( $\Delta\phi = 1$ ) when one full oscillation is completed ( $\Delta t = T$ ).

At constant growth, cell age is equal to  $a = x/v$  and the phase has thus advanced by  $\Delta\phi = a/T = x/vT$  when the cell has moved the distance  $x$  relative to the growth boundary. The initial phase is given by  $\phi_0(\tau) = \tau/T'$  and the phase at  $x$  and time  $t = a + \tau$  is therefore given by

$$\begin{aligned}\phi(x, t) &= \frac{t - a}{T'} + \frac{a}{T} \\ &= \frac{x}{v} \left( \frac{1}{T} - \frac{1}{T'} \right) + \frac{t}{T'}.\end{aligned}\quad (1)$$

It is not required that the boundary is well defined. It may be taken as any point located at a constant distance from the “real” growth boundary where  $T'$  can be measured. This is an important feature since the exact location of, for instance, the boundary of the proliferating zone in Fig. 1(a) or the posterior PSM boundary in Fig. 2(a), may not be clear. In fact, any point located in the posterior PSM half can be used to define  $T'$  since cells oscillate in synchrony in this region.

The phase function in eqn (1) can be used to calculate the velocity  $c$  and wavelength  $\lambda$  of the phase waves. The wavelength is independent of the choice of reference frame. It is the shortest distance between points having identical phase values, i.e.  $|\phi(x \pm \lambda, t) - \phi(x, t)| = 1$ . Using eqn (1),

the wavelength can be obtained as

$$\lambda = \left| v \left( \frac{1}{T} - \frac{1}{T'} \right)^{-1} \right| = \frac{vT'}{|R - 1|}, \quad (2)$$

where  $R = T'/T$ . The wave velocity  $c$  follows from the fact that the phase is an exact differential of space and time, i.e.  $d\phi(x, t) = \partial_t \phi dt + \partial_x \phi dx$ . It depends on the choice of reference frame and is equal to the velocity of a constant phase value. Setting  $d\phi(x, t)$  equal to zero and using eqn (1) to evaluate the partial derivatives, one derives that the wave velocity relative to the growth boundary is given by

$$c = \left( \frac{dx}{dt} \right)_\phi = - \frac{\partial_t \phi}{\partial_x \phi} = \frac{-v}{R - 1}. \quad (3)$$

The velocity  $\tilde{c}$  relative to the stationary cells and the overall body plan can be obtained from eqn (3) by subtracting the growth rate, i.e.  $\tilde{c} = c - v$ .

Both the wavelength and the wave velocity are controlled by the ratio of the boundary period  $T'$  to the intrinsic period  $T$  through the parameter  $R = T'/T$ . The different wave manifestations that correspond to different ranges of  $R$  are summarized in Table 1 in the reference system where the growth boundary is stationary. They are: stationary waves ( $c = 0$ ) for  $R = \infty$ , upstream traveling waves ( $c < 0$ ) for  $R > 1$ , homogeneous oscillations ( $c = \infty$ ) for  $R = 1$ , and downstream traveling waves ( $c > 0$ ) for  $R < 1$ . Note that the wave velocity must equal zero in the reference frame of stationary cells, i.e.  $\tilde{c} = 0$ , in order to form a segment-defining pattern. This is only the case if  $R$  equals zero and the periodic process must thus be arrested ( $T = \infty$ ).

Equations (2) and (3) describe the simplest possible waves formed when the parameters  $v$ ,  $T'$  and  $T$  are constant. However, these parameters depend in general on intra- and extracellular factors. One then needs to evaluate the evolution of the phase given by

$$\begin{aligned}\phi(a) &= \phi_0(t - a) + \Delta\phi(a) \\ &= \int_0^{t-a} T'(\tau)^{-1} d\tau + \int_{t-a}^a T(\tau)^{-1} d\tau,\end{aligned}\quad (4)$$

TABLE 1  
The types of FDO waves that arise for constant parameters

$R$	$c$	$\lambda$	
$\infty$	0	$vT$	Stationary relative to growth boundary
$> 1$	$-v/(R-1)$	$vT'/(R-1)$	Upstream traveling
$= 1$	$\infty$	$\infty$	Homogeneous oscillation
$< 1$	$v/(1-R)$	$vT'/(1-R)$	Downstream traveling
$= 0$	$v$	$vT'$	Stationary relative to individual cells

Note:  $R = T'/T$  where  $T'$  and  $T$  are the period at the growth/flow boundary and the intrinsic period, respectively.  $v$  is the growth/flow rate,  $c$  is the wave velocity relative to the growth/flow boundary, and  $\lambda$  is the wavelength.

where the first integral is the initial phase value ( $\phi_0$ ) and the second integral ( $\Delta\phi$ ) gives the number of cycles completed by  $a$  since it was added to the growing form. The relation between distance  $x$  and cell age  $a$  is given by

$$x(a) = \int_t^{t+a} v(\tau) d\tau. \quad (5)$$

Note that the phase in eqn (4) evolves independently of the distance from the growth boundary when the oscillation is cell-intrinsic and  $T$  is independent of  $x$ .

## 2.2. EXPERIMENTAL VERIFICATION

The predictions in Table 1 were verified in a chemical flow system where the elements of the oscillatory medium are volume elements instead of individual cells. We employed the oscillating ferroin-catalysed Belousov-Zhabotinsky reaction medium (Field, 1985) that oscillates between a reduced, red and an oxidized, blue state. The oscillating medium was peristaltically pumped against the gravity through a glass tube filled with glass beads to establish a uniform plug-flow profile. This flow reactor was fed by the outflow from a continuously stirred tank reactor (CSTR) whose period  $T'$  could be changed independently of the period  $T$  of volume elements in the flow reactor (see Kærn & Menzinger, 1999; Kærn *et al.*, 2000, for details).

Figure 3 shows four representative illustrations of (a) stationary, (b) upstream traveling waves, (c) homogeneous oscillations and (d) downstream traveling waves observed for  $R = \infty$ ,

$R > 1$ ,  $R = 1$  and  $R < 1$ , respectively. The number of frames, stacked successively from left to right, is such that a volume element entering the flow-reactor at the lower left corner exits at the upper right corner, i.e. it moves along the diagonal line in Fig. 3(a). The wavelength and wave velocity were found (Kærn *et al.*, 2000) to be in quantitative agreement with the predictions in eqns (2) and (3).

The waves observed during somitogenesis (Fig. 2) are evidently not of the simple type summarized in Table 1 and observed in Fig. 3. We therefore performed additional experiments in which the oscillation period  $T(a)$  increases [ $R(a)$  decreases] as volume elements are carried downstream and away from the inflow at a constant rate. This was achieved by gently heating the

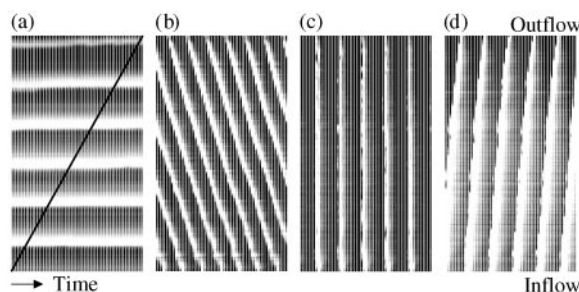


FIG. 3. Experimentally observed FDO waves in a chemical flow system. Space-time plots obtained by horizontally stacking successive images of the vertical flow reactor. The inflow is the bottom and the number of frames corresponds to a volume element carried from lower left to the upper right corner, i.e. along the diagonal line in (a). The waves were obtained by varying  $R$  at constant flow velocity ( $v = 0.102$  cm/s). 61 frames, taken at intervals of 10 s, showing 63 cm of the flow-reactor, are displayed. (a)–(d) shows, respectively, a stationary wave, an upstream traveling wave, an homogeneous oscillation and a downstream traveling wave.

CSTR and allowing for free cooling of the flow reactor such that the temperature, and hence the oscillation frequency  $1/T(a)$ , decreases as the medium moves downstream. A temperature gradient is established due to the free cooling of volume elements and the oscillation period thus depends on the time a volume element has spent in the flow reactor. Consequently, the evolution of the oscillation phase follows eqn (4) with an age-dependent value of  $T$ .

Space–time plots of phase waves observed in two experiments employing a 300 ml and a 84.2 ml CSTR shown in Fig. 4(a) and (b), respectively. The number of frames displayed in Fig. 4(a) corresponds to a volume element entering at the lower left corner and exiting at the upper right corner, thus moving along the diagonal line. The oscillation period increases in this volume element as indicated by the increasing distance between the ticks on the diagonal line. With the large CSTR [Fig. 4(a)], the FDO mechanism manifests as a homogeneous oscillation in the lower part of the flow reactor near the inflow. This oscillation periodically initiates blue oxidation bands (white in Figs 3 and 4) that propagate downstream with decreasing velocity and narrowing width. Similar behavior was observed with the smaller CSTR [Fig. 4(b)]. However, the downstream propagating wave was not initiated by a homogeneous boundary oscillation. Instead, oxidation appears periodically at a finite distance from the inlet and initiates both a downstream and an upstream propagating wave.

While the equations for the wavelength and the wave velocity in eqns (2) and (3) are derived for a constant intrinsic period, they still provide insight into the wave behavior when  $T$  increases with the age of a volume element and its distance from the inlet. The experimental conditions in Fig. 4(a) were such that the value of  $R$  was 1 near the reactor inlet and eqns (2) and (3) predict a homogeneous oscillation [Table 1, Fig. 3(c)] corresponding to a phase wave with infinite wavelength and velocity. The value of  $R$  decreases below 1 as a volume element cools down and the intrinsic period increases. For  $R < 1$ , eqns (2) and (3) predict a phase wave that propagates downstream with finite wavelength and velocity. Hence, both the wavelength and wave velocity are predicted to decrease for

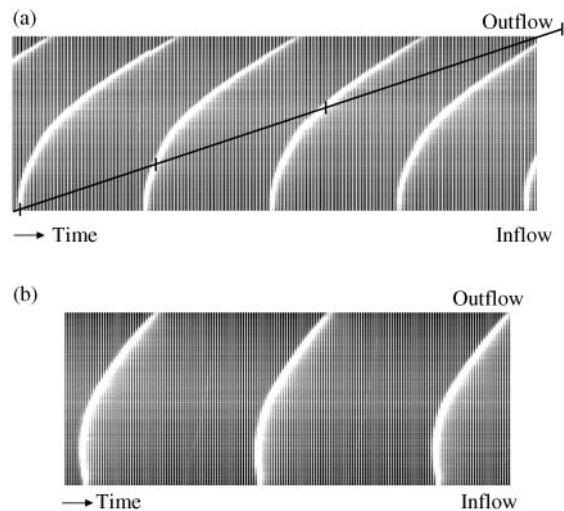


FIG. 4. Experimentally observed FDO waves when the CSTR was heated. The value of  $T$  increases as a volume element is carried through the flow reactor [diagonal line in panel (a)]. Panel (a) shows 256 frames, taken at 1 s intervals, and shows 61 cm of the flow-reactor. The number of frames is such that the volume elements entering the flow-reactor at the lower left exits in the upper right ( $v = 0.238$  cm/s). The oscillation period in this volume element is seen to increase along the diagonal line and  $R$  decreases from one at the inflow to  $R < 1$  at the outflow. Correspondingly, the lower part of the flow reactor shows homogeneous oscillations while the wavelength and velocity decrease in the downstream direction (Table 1). Panel (b) shows waves that are initiated in wave pairs at a finite distance from the inflow boundary. One wave propagates downstream and the other upstream.

decreasing  $R$  and the phase dynamics correctly predicts that the oxidation band should propagate away from the flow boundary with decreasing width and velocity.

The spatio-temporal wave behavior in Fig. 4(a) closely resembles the one observed in the chick embryo (Fig. 2) where *c-hairy1* is expressed as a homogeneous oscillation near the posterior PSM boundary and gene expression bands propagate through the PSM with decreasing width and velocity. Expression of *lunatic fringe* in the mouse (Forsberg *et al.*, 1998) appears periodically at a certain distance from the posterior PSM boundary and leads to the formation of both an anterior and a posterior propagating expression band. This behavior is similar to that observed in Fig. 4(b). The chemical flow system thus mimics the gene expression waves observed during somitogenesis in the chick and mouse.

The FDO mechanism predicts that the wavelength of the stationary pattern formed

when the intrinsic oscillation is arrested is given by  $\lambda = vT'$ . As discussed above (Fig. 2), the PSM was observed (see also Stern & Vasiliasukas, 1998) to grow by one somite length  $l$  for each completed posterior oscillation cycle. Hence, experiments indicate that the growth rate is equal to  $v = l/T'$ . In this case, the FDO mechanism predicts that the segmental pattern should have a periodicity given by  $\lambda = vT' = l$ . This is in perfect agreement with the observed periodicity of *c-hairy1* expression and the length of somites in Fig. 2.

Cooke (1998) suggested that the appearance of the gene expression waves in Fig. 2 could be due to a shortening of the length of synthesis bursts within an unaltered total oscillation time in the anterior part of the PSM. A continuously altered oscillation shape however, produces waves that are inconsistent with those in Fig. 2. To see this, consider the homogeneous oscillation in the posterior PSM half. Evidently, the homogeneous oscillation is the result of all cells having identical expression at all times. The spatial synchrony is broken when the interval expressing *c-hairy1* is altered in the anterior cells. This is however only temporal since an interval of the overall oscillation is not affected by the altered oscillation shape. As a result, and in contrast to experiments, an interval of non-synchronous expression would be followed by an interval of synchronous expression spanning the entire PSM.

### 3. FDO Model of Somitogenesis

The similar appearance of the phase waves in the biological [Fig. 2(b)] and chemical [Fig. 4(a)] systems, together with the fact that the FDO mechanism predicts the correct wavelength of the segmental pattern, supports our hypothesis that the FDO mechanism is involved in biological segmentation. In this section, we substantiate this claim by constructing an FDO model of somitogenesis in the chick and mouse. The model is intended to demonstrate that the FDO mechanism is compatible with a number of experimental observations when it is assumed that localized expression of the segmental clock genes is involved in somitogenesis. The model is not intended to be comprehensive and the

incorporation of molecular details of the segmental clock, the mechanism leading to its arrest as well as the cell-cell interactions is beyond the scope of the present investigation. Cell-cell signaling seems only to play a role in the generation of fine structure and we focus here on the cell-internally encoded aspects of somitogenesis (see discussion by Meinhardt, 1982).

The basic idea is that the spatio-temporal behavior of the gene expression waves [Fig. 2(b)] is the result of a growth-induced flow of the cells combined with the slowing down and ultimate arrest of a cellular oscillation as cells move through the PSM. The model is based on the following assumptions:

- the PSM grows by the addition of cells to its posterior boundary at a rate given by  $v(t)$ . The cells within the PSM are stationary relative to the body as a whole such that the distance to the posterior PSM boundary is given by eqn (5),
- each cell contains a segmental clock regulating a gene expression cycle. The period  $T$  of the segmental clock increases from an initial value of  $T'$  near or at the posterior boundary with increasing cell age  $a$ , and
- cells entering the PSM at the same time are at the same stage of the gene expression cycle and they age at the same rate.

We assume that the period of the segmental clock increases as cells traverse the PSM. Specifically, it is assumed that its period depends on cell age according to

$$T(a) = 1 + \exp(a - m)^k, \quad (6)$$

where the maturation parameter  $m$  determines the age at which slowing down is initiated and  $k$  determines how fast the arrest occurs. Equation (6) is expressed in dimensionless form with the period of the homogeneous posterior (boundary) oscillation taken as the unit of time ( $T' = 90$  min). While the exact location of the “organizer” leading to the synchronized posterior oscillation is not important, we assume that the cells are synchronized before entering the PSM. The intensity of gene expression is assumed to

follow  $z(\phi) = \sin[2\pi\phi(a, t)]$ , where the phase function  $\phi(a, t)$  for each cell is obtained from eqn (1). Positive and negative values of  $z$  could correspond to the expression of genes that define the anterior and posterior components of the somite. Somites form shortly after the expression of these genes has become constant. Note that  $z(\phi) = z(\phi + n)$  when  $n$  is an integer such that the gene expression oscillates with a period of one.

The FDO model implies that cells reach a state of constant gene expression, referred to as maturity, after having spent a certain amount of time in the PSM. The time taken by a cell to reach maturity is determined by the cell-intrinsic parameters  $m$  and  $k$ . They are in the simplest case constants such that the oscillation is (asymptotically) arrested when cells pass through a certain age or stage of cellular development. Our model is thus closely related to that suggested by Lewis (see Palmeirim *et al.*, 1997). The main difference lies in Lewis' *a priori* assumption of an age gradient derived from positional information. Although the model uses a different expression for the age dependence of the intrinsic period  $T$ , it would evidently be identical to the FDO model if the age gradient is established by posterior growth rather than being postulated as some preexisting positional information. The FDO model is also similar to the clock-and-trail (Kerszberg & Wolpert, 2000) and the clock-and-induction (Schnell & Maini, 2000) models. In these models however, it is a periodic process coupled to the segmental clock that is arrested and not the segmental clock itself. As will be shown in the section on somite determination, the basic FDO model can readily be expanded to incorporate a second periodic process.

### 3.1. SIMULATIONS

To study the behavior of the biological FDO model, we performed simulations in one and two spatial dimensions. In the one-dimensional simulations, each (prospective) somite was divided into  $n$  "cells" located at equidistant points separated by  $\Delta x$  along the direction of the PSM. In the two-dimensional simulations, each (prospective) somite occupied a rectangular grid composed of  $n^2$  cells. In both cases, the unit of length was taken as one somite length  $l = n\Delta x$ , the unit of

time was, as discussed above, the period of the homogeneous oscillation in the posterior PSM half that coincides with the period of somite formation [see Fig. 2(b)]. This definition of unit time allows for the elimination of the parameter  $T'$ . The growth/flow rate was constant in most of the simulations and, as indicated by Fig. 2(b), equal to one somite length per somite formed ( $v = l$ ). New cells were thus added to the PSM at intervals of  $\Delta t = 1/n$  and entered the PSM with initial phase  $\phi_0 = t$ . The phase of each cell advanced by  $\Delta\phi(a) = \Delta t/T(a)$  in each time-step [cf. eqn (4)].

#### 3.1.1. Gene Expression Waves

Figure 5 shows the spatio-temporal dynamics of the model with the gene expression displayed in tones from gray ( $z = -1$ ) to white ( $z = 1$ ). The figure shows both the reference frame in which the posterior PSM boundary is stationary and the reference frame in which the cells are stationary. This emphasizes the independence from the chosen reference frame and illustrates the qualitative agreement with the corresponding experimental space-time plots for the biological [Fig. 2(b)] and chemical [Fig. 4(a)] systems. In Fig. 5, the box [tilted in Fig. 5(a), horizontal in Fig. 5(b)] represents a group of cells (a prospective somite) or volume elements that is transported through the PSM [cf. Fig. 2(b)] or is carried away from the inflow boundary [cf. Fig. 4(a)].

The homogeneous oscillation near the inflow in Fig. 5(a) and in the posterior half of the PSM in Fig. 5(b), arises since  $R(a) = 1$  when cells are near the boundary and  $a$  is much less than  $m$ . This rapidly propagating wide band is gradually converted into a narrow band that eventually moves away from the growth/flow boundary at a velocity equal to the growth/flow rate. This is the result of a gradual arrest of the oscillation within maturing cells, i.e.  $R(a) \rightarrow 0$  for  $a \gg m$ . The distance between regions of gene expression within the stationary segmental pattern coincides, as expected, with that observed in Fig. 2. Although  $T$  remains finite for finite cell age and  $R$  is not strictly 0, the oscillation period quickly becomes so large and the velocity of the phase wave so low that the wave is stationary for all practical purposes.

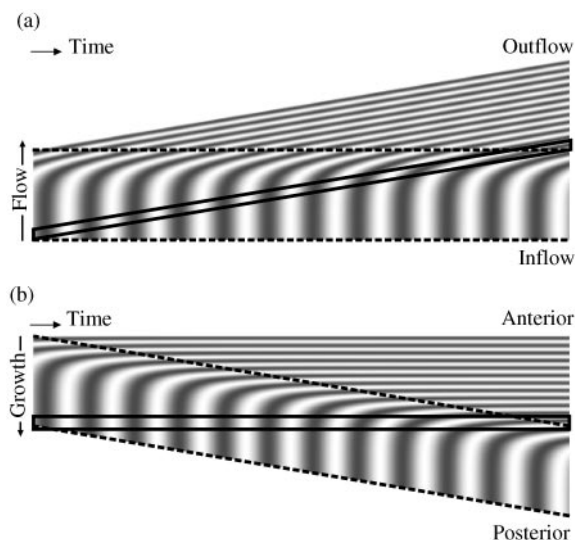


FIG. 5. Wave behavior of the FDO-based model of somitogenesis [eqns (4), (5) and (6)]. Two reference frames, corresponding to (a) a flow and (b) a growth system, are shown to emphasize the equivalence of growth and flow. The (approximate) locations of the posterior and anterior PSM boundaries are indicated by broken lines. In (a) the PSM boundaries are stationary and cells flow upward as indicated by the slanted box. In (b) the cells are stationary and posterior PSM boundary moves in the posterior (downward) direction. The homogeneous oscillation close to the inflow (a) or the posterior PSM boundary (b) is transformed into a wave that travels away from the posterior boundary with decreasing width and velocity. Eventually, the wave has velocity equal to the flow velocity in (a) while it becomes stationary in (b). The horizontal box in (b) outlines a prospective somite entering at the left and maturing to the right [cf. Fig. 4(b)]. Parameter values are  $m = 10$ ,  $k = 1$  and  $n = 30$ .

The broken lines in Fig. 5(a) and (b) outline the posterior and anterior PSM boundaries. The anterior boundary separating segmented from non-segmented mesoderm, as indicated by Fig. 2, is located where the gene expression waves have become (approximately) stationary. Clearly, the distance between the PSM boundaries remains constant. This is a natural consequence of constant growth and maturation. Each cell matures after having spent a fixed amount of time in the PSM and maturation thus takes place at a fixed distance from the growth boundary when the rate of PSM growth is constant ( $x = av$ ). Consequently, the phase wave comes to a rest at a fixed distance from the posterior boundary. The FDO model can therefore account for the relatively constant PSM length without assuming that

a signal is communicated from the anterior to the posterior boundary or that the rate of growth is coupled to the segmental clock (see Schnell & Maini, 2000).

### 3.1.2. Kinematic Segmentation

It was observed (Palmeirim *et al.*, 1998) that gene expression waves are intrinsic to the PSM and that somites are formed when the PSM is isolated from most of the surrounding tissue (Palmeirim *et al.*, 1998; Gossler & Hrabê de Angelis, 1998). Furthermore, the gene expression waves continue their predetermined program in the isolated fragments and are not disrupted when the PSM is cut transversely (Palmeirim *et al.*, 1997). These experiments indicate that the gene expression waves are phase waves that do not depend on interactions between neighboring cells. Since somites form with reversed posterior–anterior order when a fragment of the PSM is cut out and reinserted with reversed polarity (see Gossler & Hrabê de Angelis, 1998; Tam *et al.*, 2000, and references therein), somite formation is also kinematic.

The FDO model provides a natural explanation for the kinematic nature of the gene expression waves and of somite formation. As shown in Fig. 6, the FDO model readily reproduces the reversed order of segmentation when a part of the PSM is reversed. This is the result of each cell completing a fixed number of gene expression cycles such that the anterior level of expression is determined entirely by the initial level of expression  $z(\phi_0)$ . When a cell is of age  $a$ , it has completed a number of expression cycles that is given by the second integral in eqn (4). With the analytic expression in eqn (6), this integral is given by

$$\Delta\phi(a) = a + k^{-1} \ln[1 + \exp(-mk)] - k^{-1} \ln[1 + \exp(a - m)^k]. \quad (7)$$

Gene expression becomes constant when the cells have passed well beyond their maturation age. The total number of oscillations a cell will complete can thus be obtained from eqn (7) when  $a$  is much greater than  $m$ . Since  $\ln[1 + \exp k(a - m)]$

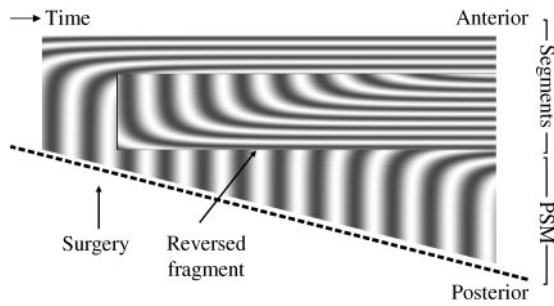


FIG. 6. Reversed segmentation in response to reversal of the PSM. The posterior PSM boundary (broken line) extends in the posterior (downward) direction. The order of the cells located within the indicated prospective somites is reversed at the time indicated by the arrow. The oscillation is slowed down and arrested in the same order as the cells entered the PSM as a result of cell-intrinsic maturation. The waves and the segmental pattern are therefore kinematic and are not affected by surgical manipulations. Parameters are the same as in Fig. 5.

$\simeq k(a - m)$  for  $a \gg m$  and  $k > 0$ , this number is given by

$$\Delta\phi(a \gg m) = m + k^{-1} \ln[1 + \exp(-mk)]. \quad (8)$$

The number of fully completed cycles  $n$  ( $n = 1, 2, \dots$ ) and the remaining fraction  $r$  ( $0 < r < 1$ ) of a cycle is determined primarily by the maturation parameter  $m$  since the second term in eqn (8) is small (about  $4.5 \times 10^{-5}$  for  $m = 10$ ,  $k = 1$ ). Each cell thus completes approximately  $m = n + r$  gene expression cycles before the segmental clock is arrested with a level of gene expression given by  $z(\phi_0 + n + r) = z(\phi_0 + r)$ . For example, when  $m$  is a relatively large integer ( $r = 0$ ) and  $z(\phi_0 + n) = z(\phi_0)$ , the mature cell expresses the same gene at the same intensity as when it entered the PSM. The expression will be phase-shifted by half a cycle when  $r = 0.5$  for  $m = 8.5, 9.5$ , etc. The fate of a given cell, that is the gene expression in the mature cell, is thus determined at the moment the cells enter the PSM and is not affected by surgical manipulations.

### 3.1.3. Segment Size

The segment size is determined by the distance between two mature cells with the same level of gene expression  $z(\phi_0 + r)$ . These cells entered the

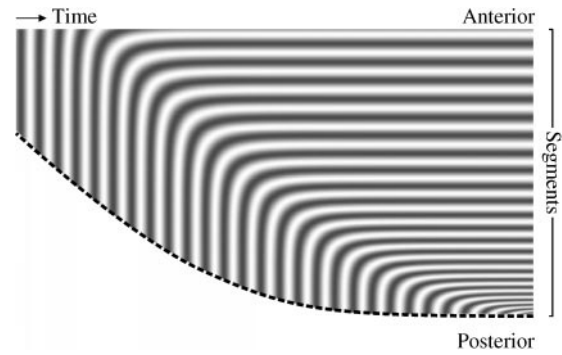


FIG. 7. Dependence of segment length on growth rate. A segmental pattern with decreasing distance between regions of expression is formed in response to slower growth towards the end of somitogenesis (tail-bud stage). The figure shows how the posterior PSM boundary (broken line) extends in the posterior (downward) direction with a growth rate  $v(t)$  that decreases linearly to zero. Initially (top right), the segments are separated by the same distance as in Fig. 5 but it decreases as growth is slowed down. Eventually, growth stops (bottom right) and somitogenesis ends when the last wave becomes stationary. The FDO model thus predicts, in agreement with experiments, that smaller somites are formed towards the end of somitogenesis.

PSM separated by a time interval of one posterior oscillation period (unit time). The distance between them thus depends on the number of cells added to the PSM during one posterior oscillation ( $\lambda = vT'$ ). Regulation of the rate of axial growth may thus provide an organism with the ability to adjust the size of segments to satisfy its specific needs. Long segments are formed at a high growth rate and short segments are formed at a low growth rate. This prediction agrees well with observations. For instance, the growth rate is high in the early stages of mouse somitogenesis while it decreases in the tail-bud stage. Correspondingly, the lumbar and sacral somites are larger and fewer while the tail somites are smaller and more numerous (Tam, 1981). As shown in Fig. 7, this is consistent with the FDO model when  $v$  decreases towards the end of somitogenesis.

It has been argued (Tam, 1981; Power & Tam, 1993), that size adaptation can be accomplished by controlling the rate of somite formation (i.e. of  $v$ ) and by adjusting the segment size (i.e.  $l = vT'$ ) proportionally, to the volume of available precursor tissue. These considerations are in perfect agreement with the FDO model. They suggest that control of  $v(t)$  [and of  $T'(t)$ ] provides an

organism with the ability to form the correct number of somites and to ensure that each of them has the correct size. For instance, if the PSM is fed by a posterior stem cell population, one would expect that this population scales with the overall size of the embryo. The rate of PSM growth would thus be reduced by a factor  $q$  in an embryo whose size is reduced by a factor  $q$ . Consequently, the segments formed in this embryo would also be reduced by a factor  $q$  and a smaller embryo would be composed of the same number of proportionally smaller segments. This is exactly what was observed in *Xenopus* when the volume of the proliferating zone was reduced at the tail-bud stage (Cooke, 1975).

### 3.1.4. Bilateral Symmetry

The PSM consists of two identical halves arranged symmetrically around the neural tube and, as shown in Figs 1(c) and 2(a), somite formation and expression of clock genes is bilaterally symmetrical and synchronous. According to Gossler & Hrabê de Angelis (1998), this ordered segmentation poses one of the major unsolved problems of somitogenesis. It seems widely accepted that the PSM halves grow at the same rate. Hence, the only assumption required for the FDO model to produce bilateral symmetry is that cells entering each of the PSM halves at the same time have more or less identical level of gene expression. This would be the case if the two halves share a common boundary and the gene expression is synchronized before or at this boundary.

Figure 8 shows a stochastic simulation of two PSM halves with a shared posterior boundary. It involves two spatial dimensions and fluctuations in the rate of posterior growth, the initial phase value as well as the cell-intrinsic parameters  $m$  and  $k$ . Clearly, the FDO model gives rise to bilaterally symmetric waves even in the presence of a fairly high level of random disturbances. As evident from Fig. 8, tight control of the cell-intrinsic maturation program is not required and the synchronization at the PSM boundary need not be perfect. Thus, bilateral symmetry does not require communication between the two PSM halves. It may readily be explained as the result of the growth rate and the initial phase

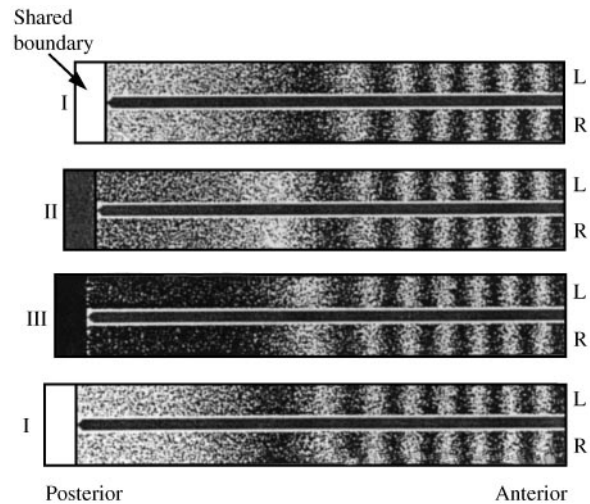


FIG. 8. Bilaterally symmetric segmentation in a stochastic FDO model. The shared boundary ensures that the two PSM halves (labeled L and R) grow at the same average rate and that cells entering each of the two halves at the same time have more or less identical phases. This leads to bilateral symmetry since each cell evolves following more or less identical programs. The average growth rate is  $\langle v \rangle = n$ , the average initial phase is  $\langle \phi_0 \rangle = t$  and the (population) averaged values of the cell-intrinsic parameters  $\langle m \rangle = 8.0$  and  $\langle k \rangle = 0.75$ , respectively. The standard deviations of the Gaussian white noise were 0.1 for all parameters and  $n = 30$ .

being coordinated at a shared posterior boundary. It is however noted that patterns without distinguishable structure were observed when the standard deviation of either the initial phase or the maturation parameter exceeds 0.5. Furthermore, the simulation in Fig. 8 uses a  $30 \times 30$  grid to represent each (prospective) somite. Evidently, the effect of noise would be greater if fewer cells were used.

The two PSM halves are derived from the same precursor tissue and indeed share a common posterior boundary (see e.g. Tam *et al.*, 2000; Pourquié, 2000, and Figs 1 and 2). Furthermore, it has been reported that the clock genes oscillate in the primitive streak (Barrantes *et al.*, 1999; Dale & Pourquié, 2000) indicating that the cells are indeed synchronized before the shared boundary. Finally, somite anomalies induced by heat shock (discussed in detail below) were most frequently formed unilaterally (Primmitt *et al.*, 1988). The reason why the two halves were affected differently is unknown (Gossler & Hrabê de Angelis, 1998) but the unilateral effect indicates that the two halves are not strongly coupled. This

in turn suggests that the same segmental mechanism operates more or less independently in the two halves. Bilateral symmetry would then arise if the two halves have identical parameters and initial conditions which, in the FDO model, may readily be accounted for, by the shared posterior boundary.

### 3.1.5. Heat Shock

Chick embryos develop multiple segment anomalies when subjected to heat shock (Primmatt *et al.*, 1988) and a single anomaly after treatment with cell-cycle-specific inhibitors (Primmatt *et al.*, 1989). The first anomaly appeared 9–10 hr after treatment and the subsequent defects followed at regular intervals of 9–10 hr coinciding with the division time  $T_M$  of cells within the PSM. The cell-cycle model (Primmatt *et al.*, 1988, 1989; Collier *et al.*, 2000), which is the only model that can account for the observations, explains the anomalies by assuming that progression through the cell cycle establishes a mitotic phase wave that is stationary relative to the posterior PSM boundary. This corresponds in the FDO formalism to  $T'_M = \infty$  and  $R = \infty$  [Table 1, Fig. 3(a)]. Cells divide at regular intervals of  $T_M = 9$  hr, which is 6 times that of somite formation. The wavelength of the mitotic wave thus spans six (prospective) somites and half the PSM length.

The cell-cycle model assumes that cell division occurs (roughly) at the center of the PSM. As cells traverse through the PSM, they pass two distinct cell cycle points  $P_1$  and  $P_2$  located on either side of M-phase and separated by 90 min in time. In essence, the model assumes that a periodically emitted signal destines cells in the  $P_1$ – $P_2$  window to form a somite. The effect of heat shock and M-phase inhibitors is to delay emission of the segment-defining signal as mitotic cells are temporally arrested and spend longer time in the PSM before passing  $P_2$ . Consequently, more cells are within the  $P_1$ – $P_2$  window when the signal arrives and the somite that forms 9–10 hr later is longer than normal (see details in Primmatt *et al.*, 1988, 1989; Collier *et al.*, 2000).

The FDO model can account for the first anomaly by requiring only one point on the cell cycle, if passage through, say,  $P_2$  causes the cellular changes leading to the arrest of the

segmental clock. The effect of delayed progression through the cell cycle would in this case cause delayed maturation of the affected cells. This can readily be modeled by increasing the value of the maturation parameter  $m$  in mitotic cells, i.e. near the center of the PSM, at the time of the treatment. In Fig. 9(a), we show the effect of increasing the value of  $m$  from 10 to 10.75 in cells with ages from 5.5 to 6.5 at the time of heat shock or by treatment with M-phase inhibitors. Figure 9 shows the first 50% of the gene expression cycle, i.e.  $0 \leq \phi(a) < 0.5$ , in dark gray while the last 50%, i.e.  $0.5 \leq \phi(a) < 1$ , is shown in light gray corresponding to the genes that are expressed in the posterior and anterior somite halves, respectively. Due to delayed maturation, the final level of gene expression  $z(\phi_0 + r)$  is phase-shifted by 75% ( $n = 10$ ,  $r = 0.75$ ) within the affected cells. Consequently, a larger-than-normal segment appears after six normal somites have formed and the subsequent segment is shorter than normal.

As many as four anomalies were observed in response to a single heat shock and the cells in the fourth anomaly do not enter the PSM until 18–20 hr after the treatment. The above mechanism, as well as the cell-cycle model, thus requires that the cells are affected long before they enter the PSM. The repeated anomalies shown in Fig. 9(a) arise when it is assumed that cells at ages from  $-6.5$  to  $-5.5$  and from  $-0.5$  to  $0.5$  are also affected by the heat shock. However, this explanation seems unlikely since some of these cells may not even exist at the time the heat shock is applied.

A more reasonable explanation for the repeated anomalies is that the heat shock affects a population of stem cells feeding the PSM. If, under normal conditions, the stem cell population fed cells to the PSM at a constant rate, the population as a whole must have a uniform distribution of cell cycle phases. Applying a heat shock causes stem cells in the mitotic state to delay their progress through the cell cycle. Consequently, there is a time interval where cell division is retarded and the growth rate is reduced. The affected cells recover from the heat shock and resume their normal division cycle after a delay. As a result, the distribution of cell cycle phases within the population will be non-uniform

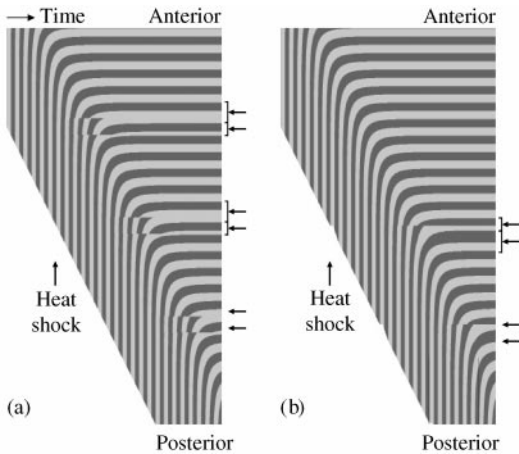


FIG. 9. Effect of heat shock or cell cycle inhibitors. The expression of two genes during the first and second half of the segmental clock, i.e. when  $z > 0$  and  $z < 0$ , are shown in dark and light gray, respectively. Panel (a) shows the effect of heat shock when passage through a point on the cell cycle initiates arrest of the segmental clock.  $m$  increases from 10 to 10.75 in cells of ages between 5.5 and 6.5. As a result, six normal, followed by two abnormal segments (arrows) are formed. Repeated anomalies from when maturation is affected in all cells in M-phase (see text). Panel (b) shows how repeated anomalies may be formed as the result of an oscillatory growth rate. The first anomaly is observed after 12 normal segments have formed and at regular intervals thereafter.

and the interval of reduced growth is followed by an interval of increased growth. It may take some time for the stem cell population to return to a uniform distribution and the effect of a single treatment may thus cause the growth rate to oscillate several times. Fig. 9(b) shows how repeated anomalies are formed when heat shock makes the growth rate oscillatory. The periodicity of the growth rate oscillation was taken to be that of the division time (9 hr = 6 time units). The first anomaly is observed after 12 normal segments have formed and an oscillatory growth rate cannot explain the formation of the first anomaly. However, the FDO model accounts well for the experimental observations when the first anomaly is the result of delayed maturation [Fig. 9(a)] and the recurrent anomalies form as the result of an oscillatory growth rate [Fig. 9(b)].

### 3.2. SOMITE DETERMINATION

#### 3.2.1. Segmental Clock

Pourquié (1999) argues that the mechanism responsible for the arrest of the segmental clock is

likely to be closely related if not identical to that determining somite polarization. Localized expression of two segment-defining genes, by the FDO mechanism may thus play a crucial role for somite polarization. The fully developed somites however contain a third distinct region that defines the boundary between posterior and anterior somite halves. A gene expression cycle that expresses only two genes, i.e. two cell states, fails to account for this region. Meinhardt (1982) solves this problem by suggesting that the oscillation consists of three states A, P and S. The segmental pattern would in this case be comprised of three regions expressing different genes corresponding to the different states of the arrested oscillation. Similarly, the FDO model may account for somite boundary formation if it is assumed that three genes are expressed during different stages of the segmental clock as shown in Fig. 10 where three cell states are manifestations of different genes expressed during different phases of the same phase wave.

The hypothesis of a segmental clock with three phases expressing different genes seems to have experimental support. It has been observed (Barantes *et al.*, 1999) that the expression of Notch pathway genes overlaps with the region where the boundary between the posterior and anterior

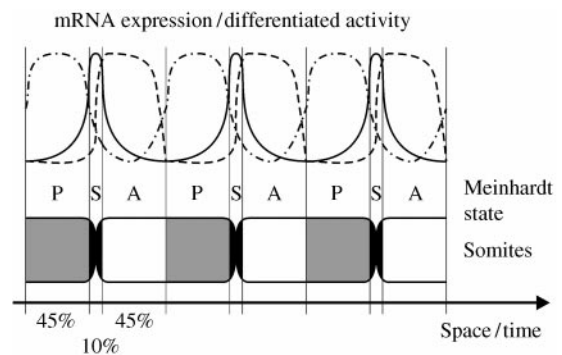


FIG. 10. Somite boundaries and polarization induced by an arrested gene expression cycle. The gene expression cycle is assumed to involve at least three genes, one for the anterior and posterior compartments and one for the somite boundary. Somite polarization and its boundaries are determined when the segmental clock is arrested and a stationary gene expression pattern is established. The segment-defining genes may not show the same dynamic expression as *hairy* since they may be activated only in the anterior end of the PSM. (-----) anterior gene; (-·-·-) posterior gene; (—) boundary gene.

halves of two consecutive somites will form. In fact, it is suggested that *lunatic fringe*, i.e., one of the clock genes, restricts the activity of *notch* to the boundary forming territory (Barrantes *et al.*, 1999). *c-hairy1* is expressed in the anterior halves and it thus seems that *hairy*, *fringe* and *notch* (or other genes that define somite polarization and boundaries) may indeed be expressed in distinct regions of the forming somites. It could, for instance, be that a boundary-defining gene is expressed in the first and last say 5% of the segmental clock cycle (black in Fig. 10). Somite boundary formation by accumulation of stable activity (Schnell & Maini, 2000) is however fully consistent with the FDO model.

The suggestion that somite boundaries, at least in part, arise from the arrest of the gene expression cycle is consistent with the observation of boundary defects in *lunatic fringe* deficient embryos (Zhang & Gridley, 1998) and that maintenance of the boundaries requires a homologue of the Notch-ligand *delta* (Hrabê de Angelis *et al.*, 1997). It thus appears that the gene expression cycle, through *notch* (Gridley, 1997; Jiang *et al.*, 1998; Lewis, 1998; Irvine, 1999; Jen *et al.*, 1999; Dale & Pourquié, 2000), is indeed linked to the formation of somite boundaries (Evrard *et al.*, 1998; Wu & Rao, 1999; Irvine, 1999; Stern & Vasiliaskas, 2000). However, as pointed out by Pourquié (1999), very little is known about the formation of somite boundaries and its relationship to anterior–posterior compartmentalization. In fact, somites are not formed without signals from the ectoderm (Palmeirim *et al.*, 1998) and somite formation is not, in contrast to segmental patterning of the PSM, intrinsic to the mesodermal tissue, at least in the chick.

### 3.2.2. Somitomers

While there is compelling evidence that somite polarization and somite boundaries are linked to the arrest of the segmental clock, the formation of metameric structures within the PSM, the somitomers (Meier, 1979), suggests that the gene expression waves are secondary since the somites-to-be appear to be defined before the stationary gene expression pattern is established. While Evrard *et al.* (1998) and Tam *et al.* (2000) argue that a somitomic pre-pattern cannot

define precise somite or half-somite units and Pourquié (1999) argues that somite polarization is linked to the segmental clock genes, the presence of somitomers prior to the formation of a stationary gene expression pattern poses a major challenge to all the models that are based on anterior determination of somite polarization and boundaries.

In the simulations in Figs 5–9, somite polarization and boundary formation was implicitly assumed to coincide more or less with the anterior PSM boundary. Cells are however destined to form a given segment at the moment they enter the PSM and it is possible that the somitomers are an early manifestation of the predetermined cell fate. In this case, there would be two mechanisms operating in parallel, one leading to somitomer formation and the other leading to localized expression of clock genes. Figure 11(a) shows a simulation where the segmental clock is shown in the left (L) PSM and somitomer formation is shown in the right (R) PSM. It is assumed that cells entering during the same posterior oscillation are allocated to a somitomer. The mechanism responsible for this could be the one suggested by the cell-cycle model and somitomers would then appear at the center of the PSM instead of at the posterior boundary as shown in Fig. 11(a).

The recent clock-and-trail model (Kerszberg & Wolpert, 2000) suggests another mechanism of internal PSM structures that may be readily incorporated into the FDO model. The entire PSM is structured in this model as the cells preserve a “snapshot” of the boundary oscillation phase at the moment they enter the PSM. Kerszberg & Wolpert (2000) argue that this could occur if a factor is synthesized during a certain phase at the PSM boundary (the progress zone) but not within the PSM. The synthesis would then stop at the moment a cell leaves the boundary and the cell would contain an imprint of the boundary phase while the segmental clock continues to oscillate. This scheme corresponds to the presence of a second process that is phase-coupled to the segmental clock at the boundary but is arrested at the moment the cells enter the PSM. In terms of the FDO formalism, this process would have a boundary period of  $T'_2 = T'$  and an intrinsic period of  $T_2 = \infty$ .

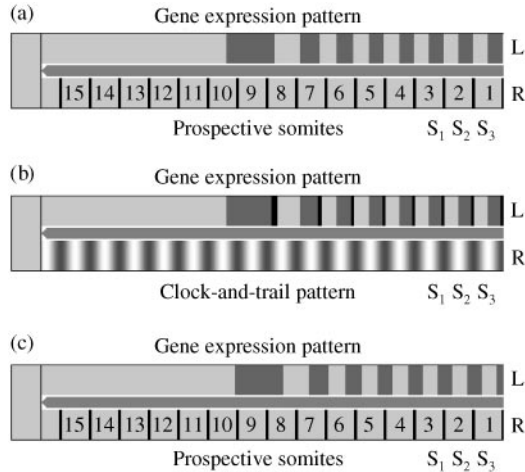


FIG. 11. Determination of somite polarization and size by two parallel mechanisms. The patterns produced by each mechanism is shown in the left (L; upper) and the right (R; lower) PSM. Panel (a) shows how the segmental clock genes may define polarization, while a second mechanism allocates cells entering the PSM during the same posterior oscillation to a somite. Panel (b) shows the co-existing gene expression patterns when the clock-and-trail model (Kerszberg & Wolpert, 2000) is incorporated into the FDO model (see text). The black stripe corresponds to a boundary-defining gene as in Fig. 10. Panel (c) shows the mismatch between cooperating mechanisms when the maturation parameter is increased by 0.3. Heat shock experiments should be able to determine whether somite size and polarization are determined by localized expression of segmental genes or by another pre-patterning process (see text).

Figure 11(b) shows a simulation where the gene expression waves are shown in the left (L) PSM and the clock-and-trail process is shown in the right (R) PSM. In this simulation, the somite polarization and boundaries are determined by the stationary gene expression wave through the mechanism outlined in Fig. 10. The right PSM indicates the level of the factor that is synthesized only at the PSM boundary such that a cell maintains the initial level of the factor as it traverses the PSM. This factor is at a high level (white) within the center of the (prospective) somites following  $y(\phi_0) = \cos(2\pi\phi_0)$  and could lead to the formation of somitomers if it increases cell-cell adhesion.

If the localized expression of clock genes is operating in parallel with a second segment-defining mechanism, it is crucial to establish which mechanism is primary and which is secondary. Unless somites are determined by a superposition of two patterns, they must be perfectly

matched. It should in this case be possible to determine which mechanism leads to somite polarization and which leads to boundary formation by monitoring how the clock genes are expressed within somites and somitomers. Figure 11(c) shows the effect of increasing the value of  $m$  by 0.3. In this case, the posterior gene (dark gray) shown in the left PSM is not restricted to the posterior end of the pattern formed by the second mechanism shown in the right PSM but it is also expressed in the anterior compartment. Mismatch between somite boundaries and the gene expression pattern within anomalous somites after, for instance, a heat shock would on one hand indicate that the localized expression of the segmental clock genes is secondary. Properly localized expression in the anterior and posterior compartments would on the other hand indicate that somites are determined by these genes and that the formation of somitomers is secondary.

#### 4. Discussion

We have presented a mechanism of wave pattern formation based on a simple physico-chemical principle and its experimental verification in a chemical system. The FDO mechanism gives rise to spatio-temporal patterns whenever an oscillating medium, i.e. a collection of self-oscillation cells, is coupled to axial growth and is temporally organized at or near the growth boundary. This mechanism may provide the organisms with the ability to express segment-defining genes in spatial patterns if, for instance, the resident stem cells in the terminal growth zone of an annelid, an arthropod or a limb bud periodically produce a factor that is not synthesized in the daughter cells. Growth-driven movement of the terminal growth zone would then leave a trail of stationary stripes within the developing form, similar to the process shown in Fig. 1(a). It is also possible that an oscillator in the plant meristem periodically initiates a leaf or a branch such that leaves or branches are shed periodically from the apical meristem as the plant elongates. This scenario corresponds in the FDO formalism to finite oscillation period  $T'$  at the boundary and to the arrest of the oscillation within the growing structure ( $T = \infty$ ,  $R = 0$ ). The

stationary phase wave formed under these conditions could allow for localized expression of segment-defining genes since different genes could be expressed during different stages of the boundary oscillation. However, an oscillator is yet to be identified in these systems and there is currently no experimental evidence for the involvement of an FDO mechanism.

The most compelling evidence for the FDO mechanism is found during somitogenesis in the chick and mouse. Posterior extension of the PSM is required for continuous somite formation (Tam *et al.*, 2000) and axial growth is an integral part of their somitogenic process [Fig. 2(b)]. Furthermore, it seems well established that cells complete a number of gene expression cycles while traversing the PSM (Palmeirim *et al.*, 1997, 1998; Stern & Vasilias, 1998; Pourquié, 2000; Stern & Vasilias, 2000) and that the gene expression is synchronized and temporally organized in the posterior PSM half or even before the cells enter the PSM (Barrantes *et al.*, 1999; Pourquié, 2000). Experimental observations thus indicate that the three conditions required for the formation of FDO waves are satisfied. Further evidence is provided by our experiments where the FDO mechanism allows a chemical flow system to mimic the spatio-temporal behavior of gene expression and from the fact that, without any assumptions, it predicts a wavelength of the segmental pattern which is in good agreement with that observed experimentally.

The above considerations indicate, that the FDO mechanism is likely to be operational during somitogenesis in the chick and mouse. To substantiate this claim, we have constructed an FDO model based on phase dynamics in a growing oscillatory medium and with age-dependent arrest of the cell-intrinsic gene expression cycle. This model offers a natural explanation for the relative constant length of the PSM, the bilaterally symmetric and synchronous segmentation and the kinematic nature of the gene expression waves and of somite formation. It also implies, in agreement with experimental observations, that the segment size can be controlled by the rate of posterior growth and that the size adaptation is a natural consequence of the growth being reduced in embryos of reduced size. Furthermore, minor assumptions allow the model to reproduce

the effect of heat shock and to offer suggestions as to how somitomeric structure and somite boundaries may be formed.

As pointed out by Tam *et al.* (2000), the gene expression patterns have not been directly matched to the (prospective) somites and there is no conclusive evidence that the pre-patterns in the PSM, such as the stationary gene expression waves or the somitomers, determine the polarization and the size of the somites. Furthermore, while some of the cycling genes have been implicated in boundary formation, somite formation is not an intrinsic property of the PSM and does not take place without the ectoderm (Palmeirim *et al.*, 1998; Pourquié, 2000). Whatever the role of the localized expression of clock genes may be, we have been unable to find any experiment indicating that they are not FDO-generated phase waves. In fact, the kinematic nature of the gene expression waves (Palmeirim *et al.*, 1997) is a strong indication that they arise as the result of phase dynamics in a growing oscillatory medium.

Our suggestion that the FDO mechanism is involved in somitogenesis is in agreement with the predictions by Meinhardt (1982) that the morphological manifestation of somites is cell-internally encoded and that cell-cell interaction (only) plays a role in the generation of fine structure during somitogenesis. The involvement of cell-cell interaction in the refinement of a basic segmental pattern is consistent with the role of the notch signalling pathway suggested by Pourquié (2000) and with the FDO mechanism. In unpublished experiments we have shown that the wavelength of FDO waves that are stationary relative to the inflow boundary can be altered by changing the strength of diffusive couplings between volume elements. It is therefore possible that an FDO model incorporating cell-cell interaction may allow cell fate as well as somite size and numbers to be altered after the cells have entered the PSM. The fact that the gene expression waves have been found to be kinematic in the chick excludes neither the involvement of cell-cell communication nor the possibility that the somite formation in general depends on or is driven by signals from the neighboring somite or the surrounding tissue. In the light that *fringe*, *notch* and *delta* encode proteins involved in transmembrane signalling, it is likely that

cell–cell interactions and stabilizing interactions between anterior and posterior somitomeric compartments play a role in somite formation, as predicted by Meinhardt (1982).

The main purpose of our model of somitogenesis is to give an example of how the FDO mechanism may provide the ability to express segment-defining genes in spatial patterns. How the somites are actually formed by such patterns cannot be captured by the FDO model or any other model of wave pattern formation that does not explicitly consider changes in physical attributes, such as cell adhesion and cell orientation, associated with segment formation. The FDO model cannot explain this aspect of somite formation but it gives, in our opinion, a plausible physical basis for the spatio-temporal gene expression waves in the PSM. In fact, the FDO mechanism is implicitly involved in many models of somitogenesis. The cell-cycle model (Primm *et al.*, 1988, 1989; Collier *et al.*, 2000) relies on a stationary FDO wave of cell cycle phases ( $R = \infty, c = 0, \lambda = vT$ ), the clock-and-trail model (Kerszberg & Wolpert, 2000) involves an imprint of the boundary oscillation ( $R = 0, c = v, \lambda = vT'$ ) and the clock-and-induction model (Schnell & Maini, 2000) employs a gradual arrest of a periodic process [ $R(a) \rightarrow 0$  for  $a \rightarrow \infty$ ] as the segmental clock completes more and more cycles. The pendulum-escapement model (Meinhardt, 1982) and the clock-and-wavefront model (Cooke & Zeeman, 1976) in its later interpretation (Palmeirim *et al.*, 1997; Cooke, 1998) also rely on the arrest of a periodic process. This recurrent theme is quite logical since it is the only way a phase wave can become stationary in the reference frame of stationary cells. Such an arrest can however occur by many different molecular mechanisms which we have yet to explore. While experiments indicate that the arrest in the chick is not induced by a reaction–diffusion mechanism, such as cell–cell signaling or a propagating wavefront, it could be induced in a cell-autonomous fashion through a counter mechanism (Schnell & Maini, 2000; Tam *et al.*, 2000), a titration mechanism (Tam *et al.*, 2000), suspended boundary synthesis (Kerszberg & Wolpert, 2000), in response to an intracellular developmental timer (Kærn & Hunding, 1998) or passage through a point on the cell cycle.

It is sometimes observed, for instance in *Xenopus*, that the segments are formed without axial growth in the early stage and during growth in the later stage of segmentation. Meinhardt (1982) suggests that early segmentation arises from the internal gradients and discusses in detail how his model can switch from gradient- to growth-driven segmentation. The only role of growth in the FDO mechanism is to generate an age and phase gradient within the developing form. However, these gradients may also be established for instance by the positional information or a morphogen gradient. The FDO mechanism is therefore consistent with traditional gradient models that do not explicitly consider axial growth an essential component of development.

## REFERENCES

- ANDRESÉN, P., BACHE, M., MOSEKILDE, E., DEWEL, G. & BORCKMANS, P. (1999). Stationary space-periodic structures with equal diffusion coefficients. *Phys. Rev. E* **60**, 297–301.
- AULEHLA, A. & JOHNSON, R. L. (1999). Dynamic expression of *lunatic fringe* suggests a link between *notch* signaling and an autonomous cellular oscillator driving somite segmentation. *Dev. Biol.* **207**, 49–61.
- BARRANTES, I. D., ELIA, A. J., WÜNSCH, K., HRABÉ DE ANGELIS, M., MAK, W. T., ROSSANT, J., CONLON, R. A., GOSSLER, A. & DE LA POMPA, J. L. (1999). Interaction between notch signalling and lunatic fringe during somite boundary formation in the mouse. *Curr. Biol.* **9**, 470–480.
- CASTETS, V., DULOS, E., BOISSONADE, J. & DEKEPPER, P. (1990). Experimental evidence of a Turing stationary structure. *Phys. Rev. Lett.* **64**, 2953–2956.
- COLLIER, J. R., MCINERNEY, D., SCHNELL, S., MAINI, P. K., GAVAGHAN, D. J., HOUSTON, P. & STERN, C. D. (2000). A cell cycle model for somitogenesis: mathematical formulation and numerical simulation. *J. theor. Biol.* **207**, 305–316.
- COOKE, J. (1975). Control of somite number during morphogenesis of a vertebrate, *Xenopus laevis*. *Nature* **254**, 196–199.
- COOKE, J. (1998). A gene that resuscitates a theory—somitogenesis and a molecular oscillator. *Trends Genet.* **14**, 85–88.
- COOKE, J. & ZEEMAN, E. C. (1976). A clock and wavefront model for control of the number of repeated structures during animal morphogenesis. *J. theor. Biol.* **58**, 455–476.
- DALE, K. J. & POURQUIÉ, O. (2000). A clock-work somite. *Bioessays* **22**, 73–83.
- EVRRARD, Y. A., LUN, T., ALUEHLA, A., GAN, L. & JOHNSON, R. L. (1998). Lunatic fringe is an essential mediator of somite segmentation and patterning. *Nature* **394**, 377–380.
- FIELD, R. J. (1985). Experimental and mechanistic characterization of bromate-ion-driven chemical oscillations and traveling waves in closed systems. In: *Oscillations and Traveling Waves in Chemical Systems*. (Field, R. J. & Burger, M., eds). New York: Wiley.

- FORSBERG, H. A., CROZET, F. & BROWN, N. A. (1998). Waves of mouse *lunatic fringe* expression, in four-hour cycles at two-hour intervals, precede somite boundary formation. *Curr. Biol.* **8**, 1027–1030.
- GOODWIN, B. C. & COHEN, M. H. (1969). A phase-shift model for the spatial and temporal organization of developing systems. *J. theor. Biol.* **25**, 49–107.
- GOSSLER, A. & HRABË DE ANGELIS, M. (1998). Somitogenesis. *Curr. Top. Dev. Biol.* **38**, 225–287.
- GRIDLEY, T. (1997). Notch signalling in vertebrate development and disease. *Mol. Cell. Neurosci.* **9**, 103–108.
- HRABË DE ANGELIS, M., MCINTYRE, J. & GOSSLER, A. (1997). Maintenance of somite borders in mice requires the delta homologue DIII. *Nature* **386**, 717–721.
- HUNDING, A. (1999). Turing structures of the second kind. In: *On Growth and Form* (Chaplain, M. A. J., Singh G. D. & McLachlan, J. C., eds), pp. 75–88. New York: Wiley.
- HUNDING, A. & ENGELHARDT, R. (1995). Early biological morphogenesis and nonlinear dynamics. *J. theor. Biol.* **173**, 401–413.
- IRVINE, K. D. (1999). Fringe, notch and making developmental boundaries. *Curr. Opin. Genet. Dev.* **9**, 434–441.
- JEN, W. C., GAWANTKA, V., POLLET, N., NIEHRS, C. & KINTER, C. (1999). Periodic repression of notch pathway genes covers the segmentation in xenopus embryos. *Genes Dev.* **13**, 1486–1499.
- JIANG, Y., SMITHERS, L. & LEWIS, J. (1998). Vertebrate segmentation: the clock is linked to notch signalling. *Curr. Biol.* **8**, 868–871.
- KÆRN, M. & HUNDING, A. (1998). Dynamics of the cell cycle engine: Cdk2-kinase and the transition into mitosis. *J. theor. Biol.* **193**, 47–57.
- KÆRN, M. & MENZINGER, M. (1999). Flow-distributed oscillators: stationary chemical waves in a flow system. *Phys. Rev. E* **60**, 3471–3474.
- KÆRN, M. & MENZINGER, M. (2000a). Pulsating wave propagation in reactive flows: flow-distributed oscillations. *Phys. Rev. E* **61**, 3335–3338.
- KÆRN, M. & MENZINGER, M. (2000b). Reply to comment on flow-distributed oscillations: stationary chemical waves in a reacting flow. *Phys. Rev. E* **62**, 2994–2995.
- KÆRN, M., MENZINGER, M. & HUNDING, A. (2000). A chemical flow system mimics gene expression waves during segmentation. *Biophys. Chem.* (in press).
- KERSZBERG, M. & WOLPERT, L. (2000). A clock and trail model for somite formation, specialization and polarization. *J. theor. Biol.* **205**, 505–510.
- KONDO, S. & ASAI, R. (1995). A reaction-diffusion wave on the skin of the marine angelfish *Pomacanthus*. *Nature* **376**, 765–768.
- KOPELL, N. & HOWARD, L. N. (1973). Horizontal bands in the Belousov reaction. *Science* **180**, 1171–1173.
- LEWIS, J. (1998). Notch signalling and the control of cell fate choices in vertebrates. *Sem. Cell. Dev. Biol.* **9**, 583–589.
- MAINI, P. K., PAINTER, K. J. & CHAU, H. N. P. (1997). Spatial pattern formation in chemical and biological systems. *J. Chem. Soc., Faraday Trans.* **93**, 3601–3610.
- MCGREW, M. J., DALE, J. K., FRABOULET, S. & POURQUIË, O. (1998). The *Lunatic fringe* gene is a target of the molecular clock linked to somite segmentation in avian embryos. *Curr. Opin. Genet. Dev.* **8**, 487–493.
- MEIER, S. (1979). Development of the chick embryo mesoblast: formation of the embryonic axis and establishment of the metameric pattern. *Dev. Biol.* **73**, 25–45.
- MEINHARDT, H. (1982). *Models of Biological Pattern Formation*. New York: Academic Press.
- MEINHARDT, H. (1999). On Pattern and growth. In: *On Growth and Form* (Chaplain, M. A. J., Singh, G. D. & McLachlan, J. C., eds), pp. 129–148. New York: Wiley.
- MIKHAILOV, A. S. (1990). *Foundations of Synergetics I. Distributed Active Systems* (Haken, H., ed.). New York: Springer-Verlag.
- MURRAY, J. D. (1993). *Mathematical Biology*, 2nd Edn. New York: Springer-Verlag.
- PAINTER, K. J., MAINI, P. K. & OTHMER, H. G. (1999). Stripe formation in juvenile pomacanthus explained by a generalized turing mechanism with chemotaxis. *Proc. Natl Acad. Sci. U.S.A.* **96**, 5549–5554.
- PALMEIRIM, I., HENRIQUE, D., ISH-HOROWICZ, D. & POURQUIË, O. (1997). Avian *hairly* gene expression identifies a molecular clock linked to vertebrate segmentation and somitogenesis. *Cell* **91**, 639–648.
- PALMEIRIM, I., DUBRULLE, J., HENRIQUE, D., ISH-HOROWICZ, D. & POURQUIË, O. (1998). Uncoupling segmentation and somitogenesis in the chick presomitic mesoderm. *Dev. Genet.* **23**, 77–85.
- POLEZHAEV, A. A. (1995). Phase waves in oscillatory media. *Physica D* **84**, 253–259.
- POURQUIË, O. (1999). Notch around the clock. *Curr. Opin. Genet. Dev.* **9**, 559–565.
- POURQUIË, O. (2000). Segmentation of the paraxial mesoderm and vertebrate somitogenesis. *Curr. Top. Dev. Biol.* **47**, 81–105.
- POWER, M. A. & TAM, P. P. L. (1993). Onset of gastrulation, morphogenesis and somitogenesis in mouse embryos displaying compensatory growth. *Anat. Embryol.* **187**, 493–504.
- PRIMMETT, D. R. N., STERN, C. D. & KEYNES, R. J. (1988). Heat shock causes repeated segmental anomalies in the chick embryo. *Development* **104**, 331–339.
- PRIMMETT, D. R. N., NORRIS, W. E., CARLSON, G. J., KEYNES, R. J. & STERN, C. D. (1989). Periodic segmental anomalies induced by heat shock in the chick embryo are associated with the cell cycle. *Development* **105**, 119–130.
- SASSONE-CORSI, P. (1998). Molecular clocks: mastering time by gene regulation. *Nature* **392**, 871–874.
- SCHNELL, S. & MAINI, P. K. (2000). Clock and induction model for somitogenesis. *Dev. Dyn.* **4**, 415–420.
- STERN, C. D. & VASILIAUSKAS, D. (1998). Clocked wave expression in somite formation. *Bioessays* **20**, 528–531.
- STERN, C. D. & VASILIAUSKAS, D. (2000). Segmentation: a view from the border. *Curr. Top. Dev. Biol.* **47**, 107–129.
- TAM, P. P. L. (1981). The control of somitogenesis in mouse embryos. *J. Embryol. Exp. Morph.* **65**, 103–128.
- TAM, P. P. L., GOLDMAN, D., CAMUS, A. & SCHOENWOLF, G. C. (2000). Early events of somitogenesis in higher vertebrates: allocation of precursor cells during gastrulation and the organization of a meristic pattern in the paraxial mesoderm. *Curr. Top. Dev. Biol.* **47**, 1–32.
- THOENES, D. (1973). “Spatial oscillations” in the Zhabotinsky Reaction. *Nature Phys. Sci.* **243**, 18–20.
- TURING, A. M. (1952). The chemical basis of morphogenesis. *Phil. Trans. Roy. Soc. London B* **237**, 37–72.

- WINFREE, A. T. (1980). *The Geometry of Biological Time*. New York: Springer-Verlag.
- WOLPERT, L. *et al.* (1999). *Principles of Development*. Oxford: Oxford University Press.
- WU, J. Y. & RAO, Y. (1999). Fringe: defining borders by regulating the notch pathway. *Curr. Op. Neurobiol.* **9**, 537–543.
- ZHANG, N. A. & GRIDLEY, T. (1998). Defects in somite formation on *lunatic fringe* deficient mice. *Nature* **394**, 374–377.